

Calculating initial data for the conformal Einstein equations by pseudo-spectral methods

Jörg Frauendiener
 Institut für Theoretische Astrophysik,
 Universität Tübingen,
 Auf der Morgenstelle 10,
 D-72076 Tübingen,
 Germany

June 12, 2021

Abstract

We present a numerical scheme for determining hyperboloidal initial data sets for the conformal field equations by using pseudo-spectral methods. This problem is split into two parts. The first step is the determination of a suitable conformal factor which transforms from an initial data set in physical space-time to a hyperboloidal hypersurface in the ambient conformal manifold. This is achieved by solving the Yamabe equation, a non-linear second order equation. The second step is a division by the conformal factor of certain fields which vanish on \mathcal{J} , the zero set of the conformal factor. The challenge there is to numerically obtain a smooth quotient. Both parts are treated by pseudo-spectral methods. The non-linear equation is solved iteratively while the division problem is treated by transforming the problem to the coefficient space, solving it there by the QR-factorisation of a suitable matrix, and then transforming back. These hyperboloidal initial data can be used to generate general relativistic space-times by evolution with the conformal field equations.

1 Introduction

In this article we shall discuss the problem of numerically calculating “hyperboloidal initial data”. These occur naturally in the numerical solution of the conformal Einstein equations, a promising approach towards the numerical evolution of general relativistic space-times [7, 8, 15, 16].

Consider an asymptotically flat solution of the Einstein equation. Let Σ be a space-like hypersurface which extends to infinity in such a way that it reaches null infinity \mathcal{J} . Assume that it remains space-like even in the limit then it will touch \mathcal{J} transversely. Prototypes for such hypersurfaces are the space-like hyperboloids in Minkowski space, hence they are called hyperboloidal hypersurfaces. These are rather different from the standard asymptotically euclidean hypersurfaces which end up at space-like infinity i^0 . In contrast to the latter hypersurfaces the hyperboloidal hypersurfaces are not Cauchy hypersurfaces of the complete space-time for the standard Einstein evolution. However, they can

still be used for pre- or retrodiction depending on whether they end up on \mathcal{J}^+ or \mathcal{J}^- .

The main reason for focusing on hyperboloidal hypersurfaces is the fact that outgoing radiation can be traced much more effectively on those hypersurfaces than it is possible on the asymptotically flat hypersurfaces [15]. This is due to the fact that they approximate a null hypersurface at large distances along which the radiation propagates instantaneously.

The initial data for the Einstein evolution on a hyperboloidal hypersurface Σ implied by the space-time geometry consists of the intrinsic metric and the extrinsic curvature. The requirement that Σ should reach out to null infinity imposes quite definite asymptotic fall-off conditions on these fields on Σ . After a suitable conformal compactification of the space-time the fall-off conditions can conveniently be captured in smoothness conditions for appropriately rescaled fields on the boundary of a three-dimensional manifold. In this “conformal” picture the evolution of initial data is most appropriately performed with the regular conformal field equations [9, 10], yielding the “conformal method” for solving Einstein’s equations. The main advantage of using this method is that the conformal field equations allow the evolution of initial data all the way up to time-like infinity i^+ , which is a regular point of the conformal manifold provided the data are sufficiently close to Minkowski data. But even if i^+ does not exist one can follow the evolution up to the point where singularities form. This has been demonstrated in [16]. Thus, it is possible to evolve the complete future of an initial hypersurface on a single grid including the points of \mathcal{J} (and even beyond, since one can smoothly extend the initial data across \mathcal{J}). This allows physically meaningful quantities like the Bondi-news and -momentum, the radiation flux etc. which well defined only on \mathcal{J} to be determined there without any further approximation, essentially by reading off the appropriate functions from the grid.

Of course, for the conformal field equations, initial data have to be determined, too. They consist no longer only of the first and second fundamental form, satisfying the standard constraint equations. The conformal field equations comprise more variables than the standard Einstein equations. In particular, they include the Bianchi identity from which follow evolution equations for both the Weyl- and the Ricci curvature. Hence, an initial data set for the evolution with the conformal field equations is larger than for the standard evolution. Such an initial data set is called hyperboloidal if the initial surface is a hyperboloidal hypersurface.

The conformal constraint equations, i.e., that part of the conformal field equations which is intrinsic to the initial hypersurface, need to be solved in order to obtain the initial data. At the moment there is no way to solve those constraints directly in more than one space dimension but there is a procedure due to Andersson, Chruściel and Friedrich [2] which allows the construction of hyperboloidal initial data. Essentially, one solves one non-linear second order equation for one scalar function to determine a conformal factor which transforms from a solution of the constraints in physical space to unphysical space. Once this has been found one can determine the remaining hyperboloidal initial data algebraically from a part of the conformal constraint equations.

In this procedure there are two complications. In the first place, the second order equation is singular at the boundary where the hyperboloidal surface intersects \mathcal{J} . Fortunately, this turns out to be more trouble for the analytical

than for the numerical treatment. And in the second place, when computing the initial data one has to divide by the conformal factor which vanishes on \mathcal{J} . Although it can be shown analytically that this “division by zero” is well defined it does pose numerical problems.

The purpose of this article is to discuss a numerical implementation for finding hyperboloidal initial data by pseudo-spectral methods and to suggest one possible way to overcome the division problem. In section 2. we describe the analytical background in more detail. The numerical solution of the second order equation is discussed in section 3 while the division problem is treated in section 4. A short discussion concludes the paper.

2 Finding hyperboloidal initial data sets

Let (\tilde{M}, \tilde{g}) be an asymptotically flat solution of the vacuum Einstein equation which has a smooth conformal structure at null infinity \mathcal{J} . Consider $\tilde{\Sigma}$, a hyperboloidal hypersurface intersecting \mathcal{J} in a smooth two-dimensional surface $\nabla\Sigma$. The Lorentz metric \tilde{g} on \tilde{M} induces a riemannian metric \tilde{h} on $\tilde{\Sigma}$. Let Ω be a conformal factor, which smoothly attaches null infinity to \tilde{M} thus defining the “conformal” space $M = \tilde{M} \cup \nabla M$. Then it follows that $\Sigma = \tilde{\Sigma} \cup \nabla\Sigma$ is a smooth submanifold with boundary in M and that $\Omega > 0$ on $\tilde{\Sigma}$ and $\Omega = 0$, $d\Omega \neq 0$ on $\nabla\Sigma$. Furthermore, there exists a smooth riemannian metric h on Σ such that on $\tilde{\Sigma}$ the relation

$$h = \Omega^2 \tilde{h} \quad (2.1)$$

holds. The embedding of $\tilde{\Sigma}$ in \tilde{M} defines the second fundamental form \tilde{k} on $\tilde{\Sigma}$. Being induced from a vacuum solution of the Einstein equation the pair (\tilde{h}, \tilde{k}) satisfies the physical constraint equations on $\tilde{\Sigma}$.

When solving the constraint equations on asymptotically euclidean initial surfaces it is convenient to make the assumption of time-symmetry, namely that the extrinsic curvature of the initial surface should vanish. This condition is not compatible with the geometry of a hyperboloidal surface but one can obtain similar simplifications in this case also by the assumption that the extrinsic curvature be pure trace, i.e., proportional to the metric,

$$\tilde{k} = \frac{1}{3} \tilde{K} \tilde{h}. \quad (2.2)$$

Then the momentum constraint implies that \tilde{K} is a constant and therefore, so is the scalar curvature ${}^3\tilde{R}$ of \tilde{h} by virtue of the hamiltonian constraint. One can assume that (after rescaling \tilde{h} with a suitable constant)

$${}^3\tilde{R} = -6. \quad (2.3)$$

Note, that the assumption (2.2) which asserts that the tracefree part of the extrinsic curvature vanishes is conformally invariant so that the extrinsic curvature of Σ in the unphysical space is also pure trace, albeit not necessarily constant.

In this paper we will impose the condition (2.2). This yields simplest case for constructing hyperboloidal initial data sets. The analytic treatment of this problem has been thoroughly discussed in [2]. But there are also several

other, less restrictive, treatments in the literature. In [1] the assumption (2.2) is dropped allowing for an extrinsic curvature which is almost general apart from the fact that the mean curvature is required to be constant. In [18] also this requirement is dropped and in [19] the existence of hyperboloidal initial data is discussed for situations with a non-vanishing cosmological constant.

In order to construct hyperboloidal initial data one may proceed as follows [11, 2]: let ω be a boundary defining function for Σ , i.e., $\omega > 0$ on Σ and $\omega = 0$, $d\omega \neq 0$ on $\nabla\Sigma$ and let h be a smooth metric on Σ . Now we seek a conformal factor Ω so that the metric $\tilde{h} = \Omega^{-2}h$ defined on $\tilde{\Sigma}$ satisfies (2.3). We write $\Omega = \phi^{-2}\omega$ for some smooth function ϕ on Σ . Then (2.3) turns into the non-linear second order equation, also called the Yamabe equation

$$4\omega^2\Delta\phi - 4\omega\nabla^a\omega\nabla_a\phi - [\omega^2R + 2\omega\Delta\omega - 3\nabla^a\omega\nabla_a\omega]\phi = 3\phi^5. \quad (2.4)$$

Here, we have used the Laplace operator $\Delta = \nabla^a\nabla_a$ with respect to h , the co-variant derivative operator ∇ and the scalar curvature R of h . The most obvious property of this equation is the fact that it degenerates on the boundary where ω vanishes. This is not entirely surprising considering its origin: if the equation were regular on the boundary one would presumably be able to specify boundary data, thus introducing some freedom into the structure of a hyperboloidal hypersurface at its intersection with \mathcal{J} . But this would be in contradiction with the fact that \mathcal{J} is universal, being fixed entirely by the smooth conformal structure. The conformal transformation properties of (2.4) ensure that the conformal factor Ω defined from a solution ϕ does not depend on the specific form of the boundary defining function ω and, furthermore, that it depends only on the conformal class of the metric h .

Consider now the following fields defined on Σ

$$\Phi_{ab} = -\Omega^{-1} \left(\nabla_a\nabla_b\Omega - \frac{1}{3}h_{ab}\Delta\Omega \right), \quad (2.5)$$

$$E_{ab} = \Omega^{-1} \left(R_{ab} - \frac{1}{3}h_{ab}R - \Phi_{ab} \right). \quad (2.6)$$

These fields are the essential initial data necessary for the evolution with the conformal field equations. Φ_{ab} is the projection of the conformal Ricci tensor onto Σ , while E_{ab} represents the rescaled electric part of the Weyl tensor. As they stand these expressions are valid only on $\tilde{\Sigma}$, being formally singular on the boundary where Ω vanishes and one needs to worry whether there exists a smooth extension to $\nabla\Sigma$. This question and the more immediate question of existence, uniqueness and regularity of solutions of (2.4) have been answered in complete detail in [2] where the following theorem has been proved.

Theorem 2.1 *Suppose (Σ, h) is a three-dimensional, orientable, compact, smooth Riemannian manifold with boundary $\nabla\Sigma$. Then there exists a unique solution ϕ of (2.4) and the following conditions are equivalent:*

1. *The function ϕ as well as the tensor fields (2.5) and (2.6) determined on $\tilde{\Sigma}$ from h and $\Omega = \phi^{-2}\omega$ extend smoothly to all of Σ .*
2. *The conformal Weyl tensor $C_{ab} = \Omega E_{ab}$ goes to zero on $\nabla\Sigma$.*
3. *The conformal class of h is such that the extrinsic curvature of $\nabla\Sigma$ with respect to its embedding in (Σ, h) is pure trace.*

Condition 3. is a weak restriction of the conformal class of the metric h on Σ , since it is only effective on the boundary. Interestingly, the theorem only requires Σ to be orientable and does not restrict the topology of Σ any further. We exploit this fact by assuming the existence of an isometric and hypersurface orthogonal action of $U(1)$ without fixed points on Σ which we take to have topology $S^1 \times S^1 \times I$. Thus, we may ignore the dependence on one coordinate, reducing the problem to one on the two-dimensional surface $S^1 \times I$. We take coordinates on this surface as $(u, v) \in [0, 2\pi] \times [-1, 1]$, with 2π -periodicity implied on the u -dependence. The boundary is given by $v = \pm 1$. In the case treated here in detail, we choose \mathcal{J} to coincide with the boundary. We refer to [24] for a more detailed discussion of space-times with these properties. In more complex cases one could think of choosing boundary functions ω which vanish not only on the boundary but also somewhere in the interior. This would define and evolve to physically interesting space-times with more complex geometries [15]. We will show one possibility below.

We choose the boundary function to be

$$\omega(u, v) = \frac{1}{2}(1 - v^2).$$

On the boundary the equation (2.4) reduces to

$$(\nabla^a \omega \nabla_a \omega) \phi = \phi^5. \quad (2.7)$$

Since ϕ has to be non-zero on the boundary this implies $\phi = \sqrt[4]{\nabla^a \omega \nabla_a \omega}$, so that the boundary values of the solution are completely fixed by the equation.

Due to our assumptions the metric on Σ has the form

$$h = h_{uu} du^2 + 2h_{uv} du dv + h_{vv} dv^2 + h_{ww} dw^2,$$

where the metric functions do not depend on the coordinate w . Since we need to specify only the conformal class of a metric on Σ we may assume that $h_{ww} = 1$, leaving the other functions arbitrary except for the condition 3. of Theorem 2.1. With these assumptions, the induced metric on the boundary is

$$p = h_{uu} du^2 + dw^2,$$

and the extrinsic curvature of the boundary with respect to the metric h is proportional to

$$\lambda = (h^{uv} h_{uu,u} + h^{vv} h_{uu,v} + 2h_{uv} h^{uv}_{,u}) du^2.$$

Condition 3. requires that λ be proportional to the induced metric p which implies, that λ itself has to vanish. One possibility to satisfy this condition is to require that $h_{uv} = 0$ and $h_{uu,v} = 0$ on the boundary. It is worthwhile to point out again that the purpose of condition 3 is to ensure the smooth extensibility of the solution and the tensor fields mentioned in theorem 2.1. It is possible to find solutions of (2.4) for free data which do not satisfy condition 3.

3 Numerical solution of the Yamabe equation

We have implemented a numerical scheme for the solution of (2.4) based on pseudo-spectral methods.

In this section we want to describe a numerical scheme based on pseudo-spectral methods for solving the Yamabe equation. There are various reasons for considering these methods. They are known for their high accuracy, at least in situations where the solution is smooth. Then the numerical error decreases exponentially with the number of degrees of freedom (i.e., the number of collocation points or the number of basis functions used to approximate the solution). This is much faster than the error decay in any finite difference method which is $O(N^{-q})$ with q usually less than 4. This property makes pseudo-spectral methods ideally suited for elliptic problems. Pseudospectral methods have been employed successfully in various areas of physics and applied mathematics. In particular, we mention the work of S. Bonazzola and his co-workers e.g., [3] on various applications in relativistic astrophysics.

Let us briefly describe the basic idea behind the use of spectral and pseudo-spectral methods. For more information on these methods we refer to the standard textbooks [5, 6, 14]. When solving a partial differential equation (time independent for our immediate purposes) in some domain Σ

$$\mathcal{L}f = 0 \tag{3.1}$$

where \mathcal{L} is some non-linear differential operator one seeks a solution in the form of an expansion in some suitable basis functions (assumed to be a complete set on the region of interest)

$$f(x) = \sum_{n=1}^N f_n \phi_n(x). \tag{3.2}$$

The most popular functions in use are the trigonometric polynomials e^{imx} and the Chebyshev polynomials $T_m(x)$. The choice depends on the topology of the domain and the boundary conditions. Inserting this expansion into the PDE yields a system of equations for the expansion coefficients. There are various ways to set up these equations. Spectral methods such as the Galerkin method reexpand $\mathcal{L}(\sum_{n=1}^N f_n \phi_n(x))$ in terms of the basis functions. This is only realistic in a few cases, mostly if \mathcal{L} is constant and linear. In most other cases, the determination of the expansion coefficients of $\mathcal{L}f$ in terms of those of f is either impossible or computationally too expensive. Then one can fall back on the pseudo-spectral or collocation method: one introduces suitable collocation points x_1, \dots, x_N and then the approximate solution is forced to satisfy the equation at the inner points and the boundary conditions. This yields N equations for the N expansion coefficients.

The existence of the collocation points allows dual representations of the function f . Besides the “physical” representation based on the function values $f(x_i)$ at the collocation points there is the “spectral” representation based on the expansion into basis functions. The idea of the collocation method is to switch freely between those two representations using whichever is best to evaluate the various terms in the operator. This is made possible (at least for the Fourier and Chebyshev polynomials) by fast Fourier transformation (FFT) techniques.

The representation in coefficient space is ideally suited for efficiently and accurately evaluating derivatives. The coefficients of the derivative of a function are easily determined from the coefficients of the function either by simple multiplications or else by three term recurrence relations. Nonlinear and/or

nonconstant terms in the operator are best computed using the physical representation.

In general, the matrices which represent the spectral approximations of even the simplest linear operators are full and difficult to invert directly. Their efficient inversion can be achieved by choosing a suitable preconditioning operator (see below).

The method we employ for solving the Yamabe equation is an iterative method using a defect correction scheme. It is based on the following observations. We write equation (2.4) formally as

$$\mathcal{L}\phi = \phi^5. \quad (3.3)$$

Here, \mathcal{L} is a linear operator made up from derivative and multiplication operators. We construct a Richardson iteration procedure by writing $\phi^{n+1} = \phi^n + \delta\phi$. Inserting this into (3.3) and ignoring terms of higher order than the first in the correction term $\delta\phi$ yields

$$\mathcal{L}\delta\phi - 5(\phi^n)^4 \delta\phi = -\left(\mathcal{L}\phi^n - (\phi^n)^5\right). \quad (3.4)$$

Thus, the general procedure for solving (2.4) is the following. Suppose we have some suitable approximation ϕ^n and compute the residual $r^n = \mathcal{L}\phi^n - (\phi^n)^5$. Then solve the *linear* equation $\left(\mathcal{L} - 5(\phi^n)^4\right) \delta\phi = -r^n$ to obtain the correction $\delta\phi$ and an updated guess $\phi^{n+1} = \phi^n + \delta\phi$. With that repeat the procedure until the accuracy is satisfactory. We observe that the linear operator acting on $\delta\phi$ is also updated at each step but only by diagonal terms.

As pointed out above, for pseudo-spectral methods, the matrix representation of the operator \mathcal{L} is generally a full $N \times N$ matrix \mathcal{L}_{PS} , so that inversion is prohibitive both in terms of time and storage requirements for high N and especially in higher dimensions. However, there exists a way to circumvent this problem which is due to S. Orszag [22]: instead of inverting the pseudo-spectral representation of \mathcal{L} , we substitute a finite-difference approximation \mathcal{L}_{FD} of \mathcal{L} into the left-hand side of equation (3.4) and use this for the iteration procedure. In general, FD-approximations have sparse matrix representations, so that the iteration equation can be solved efficiently. Note, that this substitution is only made on the left-hand side of the equation while on the right-hand side the full pseudo-spectral approximation is retained. As pointed out in [22] this method allows the efficient solution of general problems with operation costs and storage not much larger than those of the simplest finite difference approximations to the problem with the same number of degrees of freedom.

In a sense this is similar to an inexact Newton method where the exact Jacobian is replaced by some approximation. Under such circumstances one cannot expect to have the full quadratic convergence of the Newton method, for which successive errors satisfy $\epsilon_{n+1} \leq K\epsilon_n^2$ for some $K > 0$. Instead, under most circumstances one can hope for linear convergence, i.e., $\epsilon_{n+1} \leq K\epsilon_n$, so that $\epsilon_n \leq \alpha^n$ for some positive $\alpha < 1$ [20].

The solution procedure outlined in the previous section is implemented as follows. The topology suggests that we expand the fields into a Fourier series

in the periodic u -direction and Chebyshev polynomials in the v -direction as in

$$f(u, v) = \sum_{m=0}^M \sum_{l=-\frac{N}{2}}^{\frac{N}{2}-1} f_{lm} e^{ilu} T_m(v). \quad (3.5)$$

We introduce the collocation points (u_i, v_k) , where $u_i = \frac{2\pi}{N}i$, $i = 0, \dots, N-1$ and $v_k = \cos(\frac{\pi k}{M})$, $k = 0, \dots, M$. Then we can switch between the physical and the spectral representation by using fast transformation techniques. The free data h_{uu} , h_{uv} , h_{vv} are specified on the collocation points subject only to the conditions $h_{uv} = 0$ and $h_{uu,v} = 0$ on the boundary. From the metric functions the connection (i.e., the Christoffel symbols) and the scalar curvature are determined in order to obtain the differential operator \mathcal{L} . As indicated above, we use both its spectral approximation as well as a finite difference approximation. In the present case, we take an approximation which is 2^{nd} -order accurate. In deriving the expression for this approximation one has to take into account that the collocation points v_k are not uniformly distributed.

The equation (3.4) is then imposed at all the interior collocation points except at the boundary, where the values for the solution determined from (2.7) are inserted. This yields a matrix of size $(N(M-1))^2$, which is sparse. The computation of the residual, i.e., the right hand side of (3.4) at each iteration step is done with the full spectral accuracy. The linear equation for the correction is solved iteratively by methods taken from the sparse matrix package LAPACK [25].

In Fig. 1 is shown the convergence behaviour for a typical run with 32

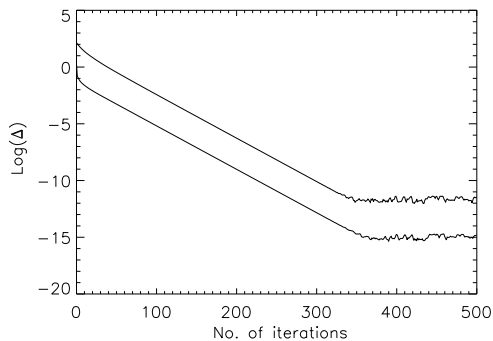


Figure 1: Size of residual and of update in the outer loop versus the number of iterations.

degrees of freedom (i.e., base functions) in each coordinate direction. The upper line is the logarithm (base 10) of the maximum size of the residual, while the lower line shows the logarithm of the maximum size of the update at each iteration step of the outer loop. Consistently, the residual is about three orders of magnitude above the update. The convergence is exponential according to the formula

$$\Delta \propto \alpha^N, \quad (3.6)$$

where we find that in this case $\alpha \approx 0.96$. The value of α depends on the number of degrees of freedom $M = 32 \cdot 33$ and the free data. As mentioned above, the convergence behaviour is not the one expected for a true Newton method. This is not too surprising since the linear operator we use for obtaining the update at each iteration step is not the Jacobian of the non-linear function. When the correction hits the level of machine accuracy no further reduction in the residual is possible and the convergence levels off, the residual remaining at a level of about 10^{-12} . The exact numbers depend on the free data.

In Fig. 3 are shown two solutions of the Yamabe equation for different kinds of free data. For the left diagram (case 1) we have chosen the following data

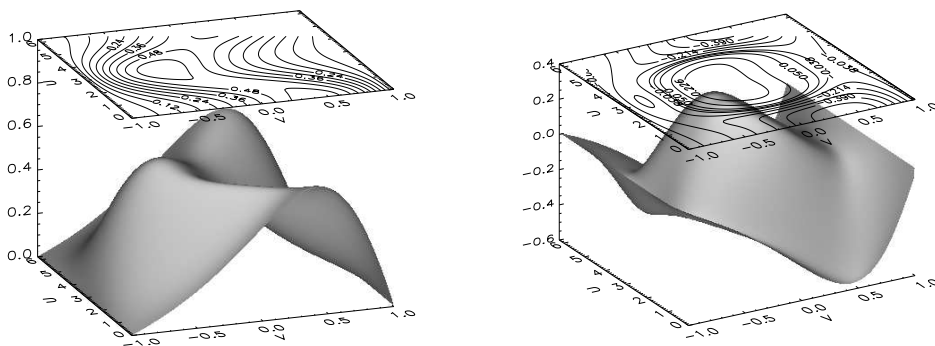


Figure 2: The conformal factor Ω obtained from the same expressions for the metric functions but different boundary functions. The region $\Omega \geq 0$ corresponds to the physical space-time.

$$\begin{aligned}\omega &= \frac{1}{2} (1 - v^2), \\ h_{uu} &= 2 \left(1 + \omega^2 (v^2 - \sin^2 u)^2 \right), \\ h_{uv} &= 2\omega (v^2 - \sin^2 u) e^{-v \cos u}, \\ h_{vv} &= 2 e^{-2v \cos u}.\end{aligned}$$

The right diagram (case 2) is meant to be a demonstration of the possibility to specify boundary functions which also vanish inside the computational grid. It was obtained by choosing

$$\omega = \frac{1}{2} (1 - v^2) \cdot \left(\frac{1}{2} (1 + \cos u)^2 + 2v^2 - 0.7 \right)$$

as the boundary function and keeping the same expressions for the metric functions. It is apparent from the contour plots that the different boundary functions correspond to different topologies of the interior regions. For case 1 there are two \mathcal{J} 's at the grid boundaries $v = \pm 1$, so that the physical space-time has the topology $S^1 \times I$, as intended. But in case 2, there are additional zeros of ω which introduce another \mathcal{J} inside the grid boundaries which has a circular topology. The resulting conformal factor defines the physical region inside that circular \mathcal{J} , giving it the topology of a disc. This two-dimensional picture is then

swept around by the $U(1)$ -action to yield a three-dimensional space-time with the topology of a full torus whose boundary is \mathcal{J} . This physical space-time is embedded in an “unphysical” region which is again bounded by a \mathcal{J} on each side.

We keep the \mathcal{J} 's at the grid boundaries because they prevent us from having to specify boundary conditions. Choosing the boundary function appropriately can lead to rather complicated space-times: by simply changing the sign of the boundary function in the example above we can switch the interior (physical) and exterior (unphysical) regions. In this way we obtain a space-time with toroidal \mathcal{J} 's and another “asymptotically flat” end, which one could loosely interpret as a black hole region. However, one should be careful with interpretations like this because we still have the assumption of the existence of a hypersurface orthogonal Killing vector.

4 The division problem

We now turn to the problem of calculating the remaining initial data from a solution of the Yamabe equation. As indicated in section 2 this involves a division of the tensor components (2.5) and (2.6) by the conformal factor. From theorem 2.1 one knows that these components vanish on \mathcal{J} and that the quotient is smooth across \mathcal{J} . Let us first discuss a one-dimensional example.

Consider two real valued functions on the interval $[-1, 1]$ with $f(0) = g(0) = 0$ and $f(x) \neq 0$, $g(x) \neq 0$ elsewhere. Our task is to compute the quotient f/g on the interval. The only problem is at the origin $x = 0$, where the quotient is not defined. Analytically, one can use l'Hôpital's rule to obtain the limit $\lim_{x \rightarrow 0} (f/g)(x)$. Numerically, however, the problem is more subtle, at least if one is interested in obtaining an answer as accurately and smoothly as possible.

Let us be more specific in our assumptions on f and g . We take them both to be at least \mathcal{C}^2 and to vanish at $x = 0$, but with $g'(0) \neq 0$. Then we have $f(x) = x\tilde{f}(x)$ and $g(x) = x\tilde{g}(x)$ for \mathcal{C}^1 -functions \tilde{f} and \tilde{g} with $\tilde{g}(0) \neq 0$. Then

$$\lim_{x \rightarrow 0} (f/g)(x) = \frac{\tilde{f}(0)}{\tilde{g}(0)},$$

but obviously this limit cannot be calculated numerically in a direct way. The limit procedure has to be realized somehow. A straightforward method would be to approximate

$$(f/g)(0) = \frac{f'(0)}{g'(0)} \sim \frac{f(\epsilon) - f(0)}{g(\epsilon) - g(0)} = \frac{f(\epsilon)}{g(\epsilon)},$$

for small enough ϵ . Unfortunately, this is only a first order approximation which, of course, could be improved by using more accurate finite difference formulae for approximating the derivatives at $x = 0$. Still, we do not get the accuracy of a spectral method.

We propose here a method which is more in line with the idea of spectral methods. Roughly speaking, we transform the problem to coefficient space, solve it there and then transform back to physical space. Define $\mathcal{T}_M = \text{span}(T_m, 0 \leq m \leq M)$, the space of polynomials on $[-1, 1]$ with degree at most M . This

space is spanned by the first $M + 1$ Chebyshev polynomials and it carries a scalar product defined by

$$\langle T_m | T_n \rangle = \int_{-1}^1 T_n(x) T_m(x) \frac{dx}{\sqrt{1-x^2}}$$

The Chebyshev polynomials are orthogonal with respect to this scalar product, but not normalized. For each $g \in \mathcal{T}_M$, multiplication by g defines a linear map $g : \mathcal{T}_M \rightarrow \mathcal{T}_{2M}$. This map and its matrix representation with respect to the basis polynomials follow from the Clebsch-Gordan like formula

$$T_n T_m = \frac{1}{2} (T_{|n-m|} + T_{n+m}). \quad (4.1)$$

Thus, e.g., the matrix representation of (multiplication by) T_0 is the $(2M + 1) \times (M + 1)$ -matrix which is the identity in the upper half and zero otherwise, while T_1 and T_2 have the following $(2M + 1) \times (M + 1)$ -matrix representations, respectively

$$\frac{1}{2} \begin{pmatrix} 1 & & & & \\ 2 & 1 & & & \\ & 1 & 1 & & \\ & & 1 & 1 & \\ & & & \ddots & \ddots \end{pmatrix}, \quad \frac{1}{2} \begin{pmatrix} & 1 & & & \\ & & 1 & & \\ 2 & & & 1 & \\ & 1 & & & 1 \\ & & \ddots & & \ddots \end{pmatrix}. \quad (4.2)$$

The higher degree polynomials T_n have similar representations. A general polynomial $g \in \mathcal{T}_M$ is a linear combination in the Chebyshev polynomials and hence its matrix representation \mathbf{G} is obtained by adding up these basic representations appropriately. Having the representation with respect to the basis polynomials it is easy to obtain the representation with respect to the normalised Chebyshev bases in \mathcal{T}_M and \mathcal{T}_{2M} .

Suppose now that f is in \mathcal{T}_{2M} . Obviously, the image of \mathcal{T}_M under multiplication by g is an $(M + 1)$ -dimensional subspace of \mathcal{T}_{2M} , hence not all $f \in \mathcal{T}_{2M}$ are also in that image. Our task is to invert the map $g : \mathcal{T}_M \rightarrow g[\mathcal{T}_M]$ on its image. Thought of in terms of linear algebra, this requires to solve $(2M + 1)$ linear equations, of which only $(M + 1)$ are linearly independent for $(M + 1)$ unknowns. The matrix \mathbf{G} is the coefficient matrix of that system of equations.

We can solve this problem by finding the reduced QR-factorisation of \mathbf{G} , i.e., we seek matrices \mathbf{Q} and \mathbf{R} so that that $\mathbf{G} = \mathbf{QR}$, where \mathbf{R} is an upper triangular $(M + 1) \times (M + 1)$ -matrix and \mathbf{Q} is a $(2M + 1) \times (M + 1)$ -matrix whose columns are mutually orthonormal. Thus, the columns of \mathbf{Q} form an orthonormal basis for the image of \mathbf{G} . It should be noted that the scalar product involved here is the one defined between the Chebyshev polynomials if one uses the normalised polynomials when representing matrices, which will be assumed in the sequel. For a more thorough discussion of the QR-factorisation from various perspectives we refer to standard textbooks on numerical linear algebra like [27, 13, 26].

Suppose now that $\mathbf{G} = \mathbf{QR}$ has been factored. We note that $\mathbf{Q}^* \mathbf{Q} = \mathbf{1}_M$, the identity in \mathcal{T}_M , while \mathbf{QQ}^* is the orthogonal projector onto the image of \mathbf{G} . Given any $f \in \mathcal{T}_{2M}$, the QR-factorisation enables us to “solve” the overdetermined system $\mathbf{G}h = f$ in the following way. We have $\mathbf{QQ}^* f = \mathbf{G}h$ for some

$h \in \mathcal{T}_M$. Hence we get $\mathbf{Q}^*f = \mathbf{R}h$ and, finally, inverting \mathbf{R} , we get h . It is a well known property of the QR-factorisation that it allows the solution of least squares problems, i.e., given the overdetermined equation $\mathbf{G}h = f$, the “solution” $h = \mathbf{R}^{-1}\mathbf{Q}^*f$ has the property that it minimizes $\|\mathbf{G}h - f\|^2$. Thus, e.g., if f is in the image of \mathbf{G} then h is the (unique, if \mathbf{R} is invertible) vector in \mathcal{T}_M for which the equation holds. But if f is not in the image, then h will be that vector in \mathcal{T}_M whose image is closest to f , i.e., for which $f - \mathbf{G}h$ is orthogonal to the image. Therefore, the QR-factorisation serves to compute the “generalized inverse” or Moore-Penrose inverse of a matrix [23].

Now we can find the solution of the division problem as follows. Given a smooth function f on the interval $[-1, 1]$ we compute its expansion into Chebyshev polynomials up to degree M . Then we can consider f to be an element of \mathcal{T}_M . We may also regard it as being in \mathcal{T}_{2M} by taking the coefficients of the polynomials with degree higher than M to be zero. We also expand the divisor g , another smooth function on the above interval and from its expansion coefficients we construct the matrix \mathbf{G} . Then we compute the QR-factorisation of \mathbf{G} by standard methods (we take Householder reflections). The solution (f/g) is obtained by computing $y = \mathbf{Q}^*f$, solving $\mathbf{R}y = z$ by back substitution and, finally, by transforming back from the expansion coefficients contained in the vector z to the function (f/g) .

Let us illustrate the above mentioned behaviour by an example. We take $g(x) = x$ and $f(x) = \sin(10x) + 2\cos(5x) - 2$. Since $f(0) = 0$, f is divisible by g with $(f/g)(0) = 5$. In Fig. 3 is shown the exact quotient (solid line)

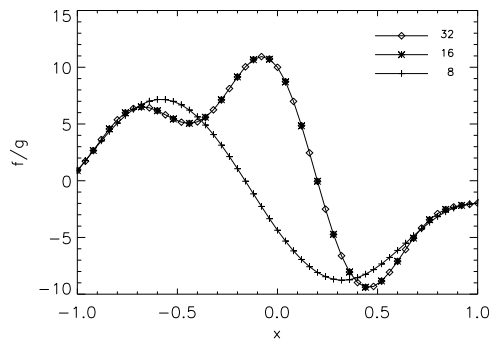


Figure 3: The quotient (f/g) (see text)

and three approximations for $h = (f/g)$ with $M = 8, 16, 32$ obtained by the procedure given above. Obviously, the lowest approximation with $M = 8$ is not usable. The reason for this is that there is too much structure present in f to be resolved with only 8 polynomials. Following the discussion in [21] and [14], we find that in this case we need about 10 polynomials to have enough resolution power, and indeed, the approximation with 16 polynomials is almost indistinguishable graphically from the exact function. With 32 polynomials the residual $\|f - h \cdot g\|_\infty$ is on the level of the machine precision, see Table 4. To illustrate the behaviour when f is not in the image of g , we take $f(x) = 1$ and $g(x) = x$. The result is shown in Fig. 4 for $M = 32$. The thin line is the

M	$\ f - h \cdot g\ _\infty$
8	1.64
16	2.19(-3)
32	3.12(-14)

Table 1: Maximum residual for approximations with different number M of polynomials.

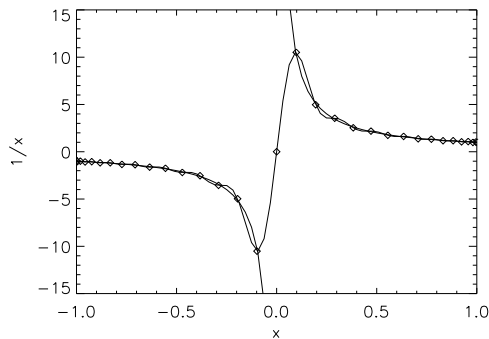


Figure 4: The quotient $1/x$ (see text)

exact function $1/x$ while the thick line is the computed approximation h . The markers indicate the values at the collocation points $x_k = -\cos(k\pi/M)$, where the approximation is very good. However, inbetween the collocation points the agreement is bad because of the high-frequency oscillation. The maximal residual is in this case $\|1 - x \cdot h\|_\infty = 1.0$, which is the value of f at the zero of g . But the maximum value of h is much higher, $\|h\|_\infty = 10.52$, one order of magnitude above the value of f at the zero of g .

In this case the zero was in the center of the interval. If, instead, g vanishes at the boundary, then the singular behaviour is much more prominent. This is due to the clustering of the collocation points towards the end of the interval which normally is a benefit, because it allows a much more accurate approximation of functions there. In our case it means a good approximation of the singular behaviour. If we take $f(x) = 1$ but $g(x) = 1 - x$ then we obtain a quotient with a maximum value of 373.9, more than two orders of magnitude above the value of f at the zero of g .

If we compute (f/g) numerically from a function f which is known analytically to have common zeros with g , but has been obtained by numerical means then f will in general not vanish exactly at the zeros of g . At those points its value ϵ will depend on the accuracy of the algorithm used to compute f . Thus, we will have $f(x) = g(x)h(x) + \epsilon$ (assuming for the moment that g has only one zero). Then, using the procedure described above, we would obtain h together with some additional “singular” or “high-frequency” part, which contaminates the result because its maximum value can be several orders of magnitude beyond the value of ϵ . The reason for this is that f is projected orthogonally onto

the image of g . But we are not so much interested in the orthogonal projection but rather we seek a projection which annihilates that high-frequency part.

This can be achieved by a simple alteration of the projector $\mathbf{P} = \mathbf{Q}\mathbf{Q}^*$ in the following way. We seek a projector $\tilde{\mathbf{P}}$ which has the same image as \mathbf{P} but which annihilates a vector, say y . We make the ansatz

$$\tilde{\mathbf{P}}z = \mathbf{P}z - \langle a|z\rangle\mathbf{P}y, \quad (4.3)$$

where a is some vector with $\langle a|y\rangle = 1$. For this to be a projector we need in addition that $\langle a|\mathbf{P}z\rangle = 0$ for all z . Thus, a is orthogonal to the image and the simplest choice for it is

$$a = \frac{y - \mathbf{P}y}{\|y - \mathbf{P}y\|^2}. \quad (4.4)$$

Inserting the expression for $\mathbf{P} = \mathbf{Q}\mathbf{Q}^*$, one readily finds

$$\tilde{\mathbf{P}}z = \mathbf{Q} \left[\mathbf{Q}^*z - \frac{\langle y|z\rangle - \langle \mathbf{Q}^*y|\mathbf{Q}^*z\rangle}{\langle y|y\rangle - \langle \mathbf{Q}^*y|\mathbf{Q}^*y\rangle} \mathbf{Q}^*y \right]$$

Now it is clear what to do numerically. First the vector y is determined as the expansion coefficients of 1 with respect to the normalised Chebyshev polynomials and, once the QR-factors of \mathbf{G} have been found, the denominator of the factor above is computed. Then each dividend is Chebyshev expanded to get the vector z of its expansion coefficients, the term in brackets above is computed and, finally, the solution is obtained by inverting \mathbf{R} . If this procedure is applied to find $1/x$ as before, then one obtains exactly zero. And in case one tries to find $(f(x) + \epsilon)/g(x)$ the result is the same no matter what value of ϵ .

So far, this procedure works only for the case where g vanishes at a single point. If there are more zeroes of g present then the procedure has to be modified. This modification is straightforward. For two vectors y_1, y_2 to be annihilated, we have the altered projection

$$\begin{aligned} \tilde{\mathbf{P}}z = \mathbf{P}z + \frac{1}{V_{12}} (\langle y_2^\perp|z\rangle\langle y_2^\perp|y_1^\perp\rangle - \langle y_1^\perp|z\rangle\langle y_2^\perp|y_2^\perp\rangle) \mathbf{P}y_1 \\ + \frac{1}{V_{12}} (\langle y_1^\perp|z\rangle\langle y_1^\perp|y_2^\perp\rangle - \langle y_2^\perp|z\rangle\langle y_1^\perp|y_1^\perp\rangle) \mathbf{P}y_2, \end{aligned} \quad (4.5)$$

where $V_{12} = \langle y_1^\perp|y_1^\perp\rangle\langle y_2^\perp|y_2^\perp\rangle - \langle y_2^\perp|y_1^\perp\rangle^2$ and where $y^\perp = y - \mathbf{P}y$ is the part of y , orthogonal to the image of \mathbf{P} . In principle, this can be generalized to even more y 's but the formulae become more and more complicated. The meaning of the vectors y_i is the following. Suppose g has n zeros in the interval. Then it is described by a polynomial of degree n . Each function in the image of \mathbf{G} is then necessarily a polynomial of degree at least n . Therefore, the projection onto the image of \mathbf{G} has to annihilate all the lower degree polynomials. This implies that one can take the standard basis vectors $(1, 0, \dots)$, $(0, 1, 0, \dots)$, \dots for the vectors y .

Let us now describe how to implement this method of division. We assume that a solution ϕ of the Yamabe equation has been obtained. Together with the boundary defining function ω it defines the conformal factor $\Omega = \omega\phi^{-2}$. Since $\phi > 0$, both Ω and ω vanish at exactly the same points. From ϕ and the geometry of Σ one determines the components of the tensor fields in (2.5) and

(2.6) by differentiation and algebraic manipulations. Let ψ be any one of those components. Analytically, one knows that ψ shares the same zeroes as Ω if the free data have been specified appropriately, so that, ideally, there is no problem when dividing ψ by Ω . However, the values of ψ will never be exactly zero at the zeroes of Ω and we have the situation described above.

We now assume for simplicity that ω is a function only of v , which is the case in the first example in section 3. This assumption is easily removed. To divide ψ by Ω we divide by ω and then multiply with ϕ^2 . The function ψ is represented by a two-dimensional array. To divide this array by ω we divide it row by row, each row consisting of the values $\psi_i = \psi(u_i)$ at the points of constant $u = u_i$. The boundary function ω is Chebyshev-transformed and from its spectral representation we construct the matrix \mathbf{G} and its reduced QR-factorisation. In the example with $\omega(v) = \frac{1}{2}(1-v^2)$ there are only two expansion coefficients because ω is an even quadratic polynomial. Then we compute the projection (4.5) of the Chebyshev-transformed row ψ_i onto the image of \mathbf{G} . The two vectors y_1 and y_2 have components δ_{k0} and δ_{k1} respectively, thus being the spectral representation of the two lowest degree polynomials. The projection corresponds to the subtraction from ψ_i of an affine function $av + b$ which agrees with ψ_i at the zeroes $v = \pm 1$ of ω . Thus, the projected function vanishes on the boundary and we can divide it by inverting the QR-factors of \mathbf{G} . Performing these operations on all rows of ψ finally yields the result ψ/ω .

As an example we show in Fig. 5 a component of the rescaled Weyl tensor which involves two divisions by ω , see eqns. (2.5) and (2.6). The maximal residual is in this case $\|\psi - E \cdot \omega\|_\infty \approx 4(-16)$ which is on the level of machine accuracy. This function is obtained from the first solution of the Yamabe equa-

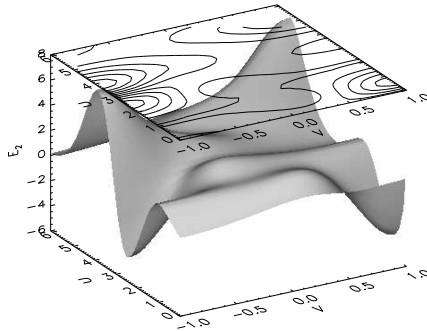


Figure 5: A component of the rescaled Weyl tensor

tion (2.4) presented in the previous section. There are no interior \mathcal{J} 's and so the boundary of space-time coincides with the boundary of the grid.

5 Conclusion

We have presented in this paper a way for obtaining hyperboloidal initial data sets for the conformal Einstein equations by using pseudo-spectral methods. It has been demonstrated that these can be efficient and powerful tools also in

numerical relativity. We have presented some results obtained under certain simplifying assumptions. In particular, these are the dimensional reduction by introducing a hypersurface orthogonal symmetry and the use of periodic boundary conditions.

Although the results presented here are encouraging there are some points to be stressed. One desirable thing for the evolution of these initial data is that they be extended beyond \mathcal{J} in a way which is as smooth as possible. This means that one has one or more \mathcal{J} 's in the interior of the grid just as in the second example presented in section 3 and then the boundary of the grid is outside the physical space-time. If the Yamabe equation is not singular at the grid boundary this means that we have to give some boundary values. These in turn influence the solution up to the inner \mathcal{J} 's while inside these \mathcal{J} 's the solution is determined from the equation alone. In general, these two parts of the solution will not match smoothly across the inner boundaries, there will be some higher derivative which jumps. This is due to the fact that the third one-sided normal derivative of the solution on \mathcal{J} is characterised by the mass aspect of that part of the region on which the derivative is taken [12]. And since there is no obvious relation between the values of the solution on the grid boundaries and the mass aspect on \mathcal{J} there is no guarantee that the third derivatives of the solution taken on either side of \mathcal{J} agree on \mathcal{J} . This implies that the initial data, and most notably the Weyl curvature, are not as smooth across \mathcal{J} as they should be.

There might be a possibility, though, to overcome this problem (due to S. Brandt [4]). If we keep the grid boundaries singular then we do not need to specify boundary conditions there. Then it might be possible that the specification of free data which are analytic enforces the equality of the mass aspects of the different regions on their common \mathcal{J} . This possibility needs to be studied in detail.

We have shown here some results in two dimensions. The generalisation of the Yamabe solver to full three dimensions should be straightforward. The situation is not so clear for the division part. The fact that the two-dimensional division is performed by stacking together one-dimensional divisions might be impractical in three dimensions.

Another limitation of the division procedure is the fact that it has to be changed whenever the boundary defining function acquires more zeros. This is more a matter of practicality than of principle. A final remark concerns the accuracy of the division method. Although each individual division can be made quite accurately with this method this does not imply that the quotients are similarly accurate, in the sense that the conformal constraint equations are satisfied to any accuracy comparable to that of the divisions. The reason for this is that the division process only ‘‘cures the symptoms’’, namely the mild non-vanishing of the dividends on the boundary. It does not remove the reason for this phenomenon. That would probably be related to the fact that the Yamabe equation does not only enforce the behaviour of the function on the boundary but also of its first derivative. This has not been used so far in the solution process of the equation. Therefore, we cannot expect that the derivative of the numerical solution has the values it should have on the boundary. And so the constraints are only satisfied to the degree with which these values are attained. This problem is currently being studied.

Thus, to summarize, we feel that the Yamabe solver can be made a rather

efficient and accurate tool, while the divisor may have its limitations. These come mostly from the fact that it cannot be easily applied for more general boundary functions. There is a completely different approach to the division problem developed by Hübner [17], where one solves a linear elliptic equation for the quotient ψ/ω which is singular at $\omega = 0$.

The results and methods presented in this paper demonstrate the feasibility of numerically determining initial data sets for the conformal field equations along the lines of [1, 2]. They enable the numerical evolution of general relativistic space-times using the “conformal method”.

Acknowledgments

It is a pleasure to thank the members of the mathematical relativity section of the MPI für Gravitationsphysik in Potsdam. I am particularly grateful to H. Friedrich and P. Hübner for useful discussions on the analytical and numerical intricacies of the Yamabe problem. Furthermore, I wish to thank S. Bonazzola for letting me have a look into his pseudo-spectral hydro-code where I found some very useful tricks and techniques. This work is funded by the DFG grant FR-848/3.

References

- [1] L. ANDERSSON AND P. T. CHRUSCIEL, *On hyperboloidal Cauchy data for vacuum Einstein equations and obstructions to smoothness of scri*, Comm. Math. Phys., 149 (1994), pp. 587–612.
- [2] L. ANDERSSON, P. T. CHRUSCIEL, AND H. FRIEDRICH, *On the regularity of solutions to the Yamabe equation and the existence of smooth hyperboloidal initial data for Einstein’s field equations*, Comm. Math. Phys., 149 (1992), pp. 587–612.
- [3] S. BONAZZOLA, E. GOURGOLHON, AND J.-A. MARCK, *Spectral methods in general relativistic astrophysics*. this volume.
- [4] S. BRANDT, private communication.
- [5] C. CANUTO, M. Y. HOUSSAINI, A. QUARTERONI, AND T. A. ZANG, *Spectral methods in fluid dynamics*, Springer Verlag, Berlin, 1988.
- [6] B. FORNBERG, *A practical guide to pseudospectral methods*, Cambridge University Press, 1996.
- [7] J. FRAUENDIENER, *Numerical treatment of the hyperboloidal initial value problem for the vacuum Einstein equations. I. The conformal field equations*. to appear in Phys. Rev. D.
- [8] ———, *Numerical treatment of the hyperboloidal initial value problem for the vacuum Einstein equations. II. The evolution equations*. to appear in Phys. Rev. D.

- [9] H. FRIEDRICH, *The asymptotic characteristic initial value problem for Einstein's vacuum field equations as an initial value problem for a first-order quasilinear symmetric hyperbolic system*, Proc. Roy. Soc. London A, 378 (1981), pp. 401–421.
- [10] ———, *Cauchy problems for the conformal vacuum field equations in general relativity*, Comm. Math. Phys., 91 (1983), pp. 445–472.
- [11] ———, *On hyperboloidal hypersurfaces*, in Approaches to Numerical Relativity, R. d'Inverno, ed., Cambridge University Press, 1993.
- [12] ———, private communication.
- [13] G. H. GOLUB AND C. F. VAN LOAN, *Matrix Computations*, The Johns Hopkins University Press, Baltimore, 1989.
- [14] D. GOTTLIEB AND S. A. ORSZAG, *Numerical Analysis of spectral methods: Theory and Applications*, SIAM-CBMS Philadelphia, 1977.
- [15] P. HÜBNER, *Black hole spacetimes on grids with trivial boundaries*. preprint AEI-062,gr-qc/9804065.
- [16] ———, *General relativistic scalar field models and asymptotic flatness*, Class. Quant. Grav., 12 (1995), pp. 791–808.
- [17] ———, private communication.
- [18] J. ISENBERG AND J. PARK, *Asymptotically hyperbolic nonconstant mean curvature solutions of the Einstein constraint equations*. Class. Quant. Grav., 14 (1997), pp. A189–A201.
- [19] J. KÁNNÁR, *Hyperboloidal initial data for the vacuum Einstein equations with cosmological constant*, Class. Quant. Grav., 13 (1996), pp. 3075–3084.
- [20] C. T. KELLEY, *Iterative Methods for Linear and Nonlinear Equations*, SIAM, Philadelphia, 1995.
- [21] H.-O. KREISS AND J. OLIGER, *Comparison of accurate methods for the integration of hyperbolic equations*, Tellus, 24 (1972), pp. 199–215.
- [22] S. A. ORSZAG, *Spectral methods for problems in complex geometries*, J. Comp. Phys., 37 (1980), pp. 70–92.
- [23] R. PENROSE, *A generalized inverse for matrices*, Proc. Camb. Phil. Soc., 51 (1955), pp. 406–413.
- [24] B. G. SCHMIDT, *Vacuum space-times with toroidal null infinities*, Class. Quant. Grav., 13 (1996), pp. 2811–2816.
- [25] T. SKALICKÝ, *Laspack reference manual*. <http://www.tu-dresden.de/mw-ism/skalicky/laspack/laspack.html>, Dresden University of Technology, 1996.
- [26] J. STOER AND R. BULIRSCH, *Einführung in die Numerische Mathematik II*, Springer-Verlag, Berlin, 1978.
- [27] L. N. TREFETHEN AND D. BAU, *Numerical Linear Algebra*, SIAM, Philadelphia, 1997.